From Discrete Particles to Spherical Aggregates: A Simple Approach to the Self-Assembly of Au Colloids

Ziyi Zhong,*[a] Alamelu Suriya Subramanian,[a] James Highfield,[a] Keith Carpenter,[a] and Aharon Gedanken*[b]

Abstract: Here we demonstrate a simple, template-free approach to the formation of spherical gold aggregates through the reduction of $HAuCl_4$ by $NaBH_4$, in the presence of cysteine (Cys) as a capping agent. The resulting aggregates are quite stable in solution. The pH of the solution and the molar ratio of Au:Cys are two key empirical factors in the formation of such highly ordered aggregates. At slightly alkaline pH (7–10) and with Au:Cys ratios ranging from 1:0.5 to 1:2, spherical Au aggregates of 30–80 nm are formed. At lower Cys ratios (Au:Cys $\geq$ 1:0.5) very loosely linked aggregates are formed; however, at very high Cys ratios (Au:Cys $\leq$ 1:3), highly dispersed Au particles of 2–4 nm are obtained, which are virtually indistinguishable from the original colloidal form. Aggregate size is influenced markedly by component concentration; a 3-fold increase in standard levels resulted in Au spherical aggregates of a larger size, 200–500 nm. In addition, we used a combination of Cys and lysine (Lys) as a capping agent/cross-linker and found that the morphology of the Au colloid aggregates can be easily manipulated from a linear to a spherical form by adjusting the proportions of Cys and Lys in the capping agent/cross-linker mixture. The introduction of mercapto (SH)-containing organic acids reduced the cross-linking ability of Cys, especially in the case of long-chain acids. Complete disruption of the spherical aggregates highlights the importance of Cys per se. An explanation of this ordered self-assembly process is proposed, in the context of the known surface chemistry of Au colloids.

Keywords: aggregation · colloids · gold · self-assembly · surface charge

Introduction

Multiscale engineering can be exploited to facilitate the development of systems designed at the molecular level to applications of mesoscopic or macroscopic dimensions.[1] This technology is also fundamentally important because organized structures can display valuable optical and/or electrical properties distinct from those of the individual constituent particles (atoms, molecules) or of the larger solid mass.[2] In the "bricks and mortar" ("BM") strategy for the organization of large-scale Au colloids, structures such as alkanedithiols, functionalized polymers, and biomolecules provide cohesion ("mortar") for the assemblage.[3] The linkage of some biomolecules possessing unique specificity, such as single-stranded DNA or antigens, to Au may provide applications of such composites in the field of molecular recognition.[3,4] Other techniques for the controlled assembly of Au particles include the use of template molecules with defined symmetry[5] and interparticle spacing,[6] metal coordination,[7] a polymer-mediated "BM" strategy coupled with hydrogen bonding,[8] and Langmuir techniques.[9] Although some success has been achieved,[8,10] the formation of aggregates of controllable size and shape in solution remains far from routine. Particular problems are uncontrollable precipitation and latent insolubility.[11]

Recent work in this laboratory has focused on the use of amino acids as novel, water-soluble, binding agents. It has been shown[12] that the two functional groups in cysteine (Cys) (SH and NH_2) are able to bind Au particles, but with varying abilities; the SH group binds readily, whereas the amine group displays pH-dependent behavior due to

---

[a] Dr. Z. Zhong, A. S. Subramanian, Dr. J. Highfield, Dr. K. Carpenter
Institute of Chemical Engineering and Sciences
1 Pesek Road, Jurong Island, Singapore 627833 (Singapore)
Fax: (+65) 63166182
E-mail: zhong_ziyi@ices.a-star.edu.sg

[b] Prof. A. Gedanken
Department of Chemistry and Kanbar Laboratory for Nanomaterials
Bar-Ilan University Center for
Advanced Materials and Nanotechnology
Bar-Ilan University, Ramta-Gan 52900 (Israel)
Fax: (+97) 235-351-250
E-mail: gedanken@mail.biu.ac.il

DOI: 10.1002/chem.200400529 © 2005 Wiley-VCH Verlag GmbH & Co. KGaA, Weinheim

protonation/deprotonation caused by the preliminary dissociation of the neighboring carboxylic acid group. By adjusting the pH, starting concentrations, and surface charge (by way of the Au:Cys ratio), the aggregation process can be manipulated to produce a structure of desired size and shape. Another advantage of using Cys as a capping/cross-linking agent is the dispersibility in water conferred to the spherical aggregates. To our knowledge,[13] this is the first report of a method mediated by amino acids to produce spherical Au aggregates of adjustable size. This technology has many conceivable biological applications.

Results and Discussion

Influence of pH: Figure 1 shows the transition electron microscopy (TEM) images of Au aggregates prepared at a Au:Cys ratio of 1:1. At low pH (pH 4, Figure 1a) the precipitated Au aggregates possess irregular morphology. At pH 6 (Figure 1b) some cross-linking is evident, but the particle morphology remains fairly featureless. At slightly alkaline conditions ($\mathrm{pH} \geq 8$, Figure 1c) well-formed spheres with a diameter ranging from 30 to 80 nm are observed. The pH range of 7–10 appears to be optimal for quantitative yields of spherical aggregates. As shown in Figure 1d and Figure 2 (high resolution TEM image), the spherical aggregate is composed of constituent Au colloids of 2–4 nm in size, with some visible interconnectivity.

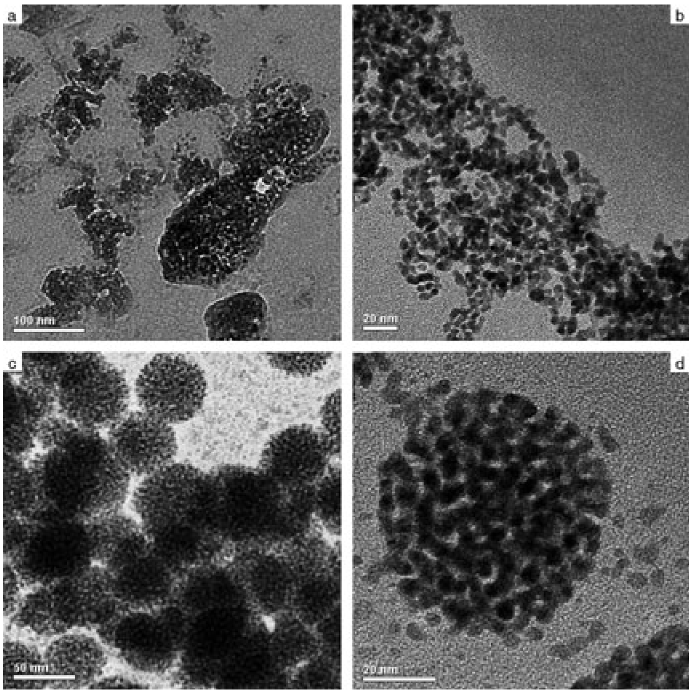

Figure 1. TEM images of Au colloids capped with cysteine molecules at various pH values (molar ratio Au:Cys = 1:1). a) pH 4.0, white bar represents 100 nm; b) pH 5.8, white bar represents 20 nm; c) pH 9.0, white bar represents 50 nm; d) magnification of the image in (c), white bar represents 20 nm.

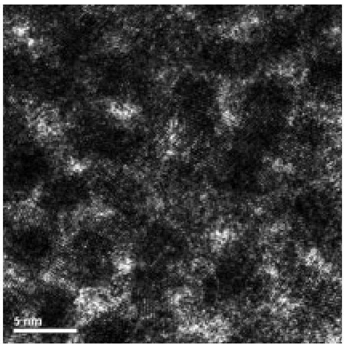

Figure 2. High resolution TEM image of the Au spherical particles shown in Figure 1d. White bar represents 5 nm.

UV-visible spectroscopy can be used to diagnose the aggregation state of Au colloids. Highly dispersed Au particles with diameters of 10–20 nm exhibit an absorbance peak of approximately 520 nm. As the Au particle size decreases to about 5 nm the extinction peak shifts to around 500 nm. However, as Au colloid size decreases to less than 3 nm, no sharp absorbance peak is observed within the UV-visible range. These phenomena are well documented,[14] and we have confirmed them for our own Au samples of different sizes, as well as for commercial Au colloidal products (Sigma).[12] If Au particles are linked or aggregated, a second extinction peak at a longer wavelength appears due to the dipole plasmon resonance of the Au nanoparticles.[15] Xu and co-workers developed the Mie theory[16] and provided detailed theoretical calculations that can be applied to different states of aggregation. Our previous calculations,[12] based on Xu's method, also confirm that the linear linking of Au nanoparticles produces a dipole plasmon resonance (second peak) within the range of 500–800 nm. This observation, however, depends heavily on aggregate size and interparticle distance; smaller aggregates and shorter interparticle distances result in a more significant peak shift towards longer wavelengths.

The UV-visible spectra of the above samples are presented in Figure 3, and their features are consistent with the microscope images. At low pH values ($\mathrm{pH} \leq 6.0$, Figure 3), the broad hump within the wavelength range 520–700 nm indicates intense aggregation among Au colloids, as shown in Figure 1a. The overall absorption is responsible for the black color of the mixture. However, with a slight increase in pH value ($\mathrm{pH} \leq 7$), the longer wavelength hump becomes weaker. Under alkaline conditions, the spectra are merely featureless continua; however their absorptions relative to each other increase progressively at wavelengths greater than 700 nm. The TEM observations above show that Au spherical aggregates form within these samples, which accounts for the continuous increase in absorbance at high wavelengths. Because these spherical aggregates are very symmetrical and have sizes within the 30–80 nm range, their absorbance curves exhibit a lack of peaks. The TEM images also reveal that the individual Au particles of these samples are quite small (2–4 nm); therefore, no optical features were observed for discrete Au colloids.

© 2005 Wiley-VCH Verlag GmbH & Co. KGaA, Weinheim

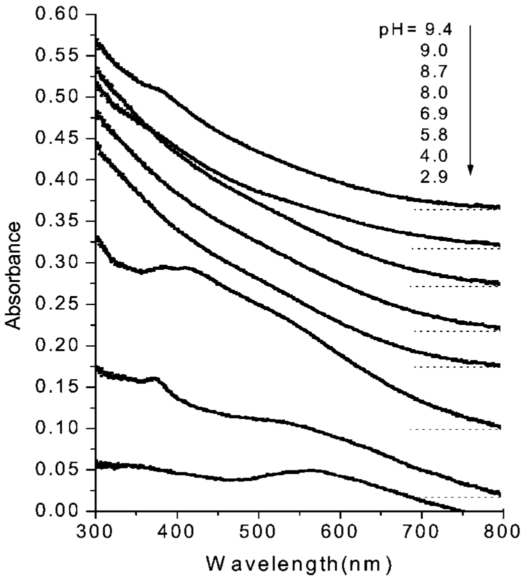

Figure 3. UV-visible spectra of Au colloids capped with cysteine molecules (molar ratio Au:Cys = 1:1) at various pH values.

Because small particles are thermodynamically unstable, they tend to aggregate together to reduce their high surface energy. As metal colloids usually possess a surface charge, the electrostatic repulsion between the Au colloids tends to prevent them from aggregating. In our investigations, the second driving force for aggregation was the cross-linking of Au colloids by Cys molecules that possess two functional, terminal groups.

Although the formation mechanism of these spherical aggregates is not fully understood, we suggest that it is based on a combination of the three forces described above. It is well known that thiol, amine, and cyanide groups bind readily to Au colloids.[17] However, as demonstrated in an earlier report,[12] the SH group in Cys binds much more readily than the NH_2 group to Au particles. Thus, the α-NH_2 group and its adjacent carboxylic acid group will project from the surface of the Au colloid (Scheme 1). At low pH values, there will be less net negative charge on the Cys molecule (believed to be responsible for hindering aggregation through interparticle repulsion), with the result that massive agglomeration inevitably results. At increasing pH, the Au colloids gradually accumulate surface negative charge, such that cross-linking becomes more difficult, as seen in Figure 1b. As the pH approaches and exceeds the pK_a value of Cys (8.5), the surface negative charge is suddenly and dramatically increased. At the same time, the amine group may be released from the hydrogen bond that it forms with its neighboring Cys molecule, which makes it more capable of binding to Au colloids (Scheme 1). As a result, spherical aggregates are formed, as this shape reduces surface free energy most effectively.[18] A detailed theoretical calculation is required to elucidate this issue. A related complicating factor is the possible oligomerization of Cys molecules on the Au colloid surfaces due to the dense packing of the former.[19]

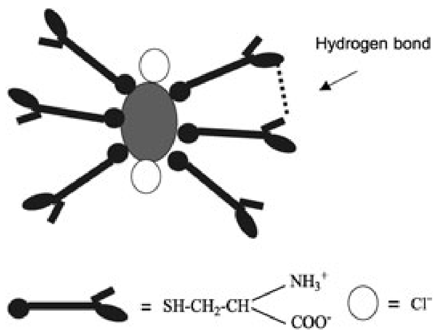

Scheme 1. Au colloid capped with Cys molecules and chloride anions. As the pH value increases, more NH_3^+ functional group ions become deprotonated; therefore, the Au colloid becomes more negatively charged. This enhances the electrostatic repulsion between the Au colloids.

Influence of Au:Cys ratio and concentration: At a fixed end-point (pH 9) and in the absence of Cys, Au colloids aggregate randomly into a three-dimensional network (Figure 4a). The introduction of Cys (Au:Cys = 1:0.5) results in a looser network, but still without a definite morphology (Figure 4b). This is probably because the amount of Cys is insufficient to enable effective cross-linking. As the molar ratio of Au:Cys increases from 1:1 to 1:2 (Figure 4c), spherical Au aggregates are formed almost exclusively; however, for

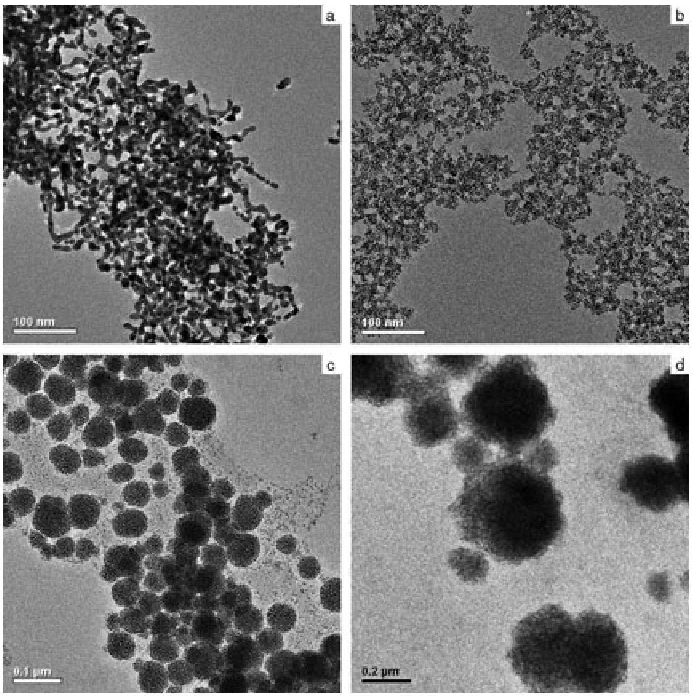

Figure 4. TEM images of Au colloids capped with Cys molecules at various molar ratios and concentrations: a) [$HAuCl_4^-$] = 1 mM, molar ratio Au:Cys = 1:0, white bar represents 100 nm; b) [$HAuCl_4^-$] = 1 mM, molar ratio Au:Cys = 1:0.5, white bar represents 100 nm; c) [$HAuCl_4^-$] = 1 mM, molar ratio Au:Cys = 1:2, white bar represents 0.1 μm; d) [$HAuCl_4^-$] = 3 mM, molar ratio Au:Cys = 1:1, black bar represents 0.2 μm. All end-point pH levels were maintained close to 9.0.

Au:Cys ratios close to 1:3, only a few large, spherical aggregates are formed, with most of the Au colloids remaining discrete (data not shown). A high surface density of Cys molecules would be expected to exert strong electrostatic repulsive forces that hinder cross-linking. A slight shrinkage in Au colloid size (to 2–3 nm) was also observed, as remarked by others.[20] In this case, it is likely that the initially formed Au clusters will be immediately capped and saturated by Cys molecules, thereby restricting subsequent Au atom deposition, preventing further colloid growth. On this basis it appears that the formation of spherical aggregates involves a subtle balance between the cross-linking ability afforded by Cys molecules and the concomitant electrostatic repulsion between the Au colloids. Evidently, only conditions favoring partial coverage by Cys can promote controlled, isotropic growth.

The UV-visible spectra obtained in the absence of Cys (Figure 5, bottom) show the characteristic Au colloid absorbance peaks at 517 nm (particle size 7–10 nm), but with an intensifying tail towards the near IR region, suggestive of strong aggregation. At a molar ratio Au:Cys of 1:0.5 a broad hump at around 520 nm suggests a "smearing out" of the individual colloid absorbance due to a loose state of agglomeration. At a ratio Au:Cys of 1:1, a relative flattening of the spectrum is observed, suggestive of spherical aggregate formation, as demonstrated in Figure 3. As the proportion of Cys increases further (Au:Cys = 1:2–1:3), the absorbance spectrum curves more sharply upwards towards the UV region (because of the increase in Cys), but remains featureless. This indicates the predominance of original (2–3 nm) Au colloids in the solution.[14]

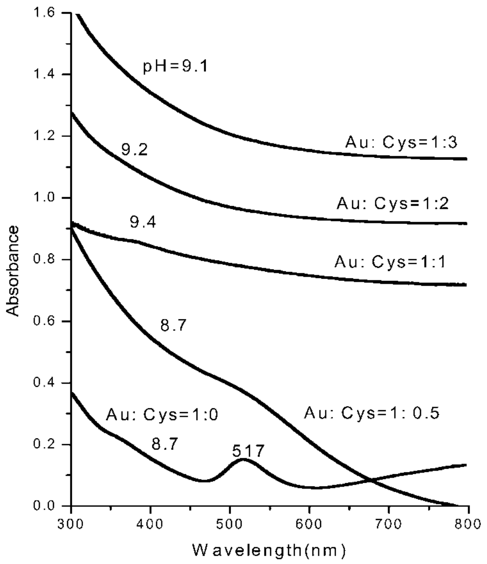

Figure 5. UV-visible spectra of Au colloids capped with Cys molecules at various molar ratios.

The concentration of reactant has a strong influence on the size of the aggregates formed, although their spherical form is maintained. A 3-fold increase in the concentration of all components at a fixed Au:Cys ratio (1:1) results in much larger spherical aggregates within the range 200–500 nm, as shown in Figure 4d. A 10-fold increase in concentration produces a further increase in aggregate size, and high resolution transition electron microscopy (HRTEM) observations of these spherical aggregates show that they are still composed of colloidal Au subunits. These massive spherical aggregates are, unfortunately, less stable than the smaller ones produced at "standard" concentrations. Such a high density of colloids in solution results in precipitation within 30 min, in contrast to standard preparations, which required longer than one month before precipitation occurred.

From linear to spherical aggregates: Previously,[21] we reported that Au nanowires can be synthesized by using lysine (Lys) as a capping agent, within a pH range of 8–10. Adjustment of the morphology of the Au aggregates may, therefore, be possible by mixing Cys and Lys in specific proportions. By using the trial Au:Cys:Lys ratio of 1:0.2:0.8, the Au colloids were seen to assemble into chain-like structures. However, the "chain cross-section" consists of several Au colloids (Figure 6a), not a single colloidal subunit, as would result from the use of Lys alone.[21] As the ratio of Cys:Lys was increased (with the ratio of Au:(Cys + Lys) fixed at 1:1), the Au colloid aggregates became progressively more rounded in shape, as shown in Figure 6b and c. At the point at which Cys was the sole capping agent, very symmetrical spherical aggregates were obtained, as illustrated and discussed above (Figure 1c). This systematic trend, that is, the expression of both functionalities, is rather surprising in view of the relative dimensions of the two capping agents; Cys has a two-carbon chain, whereas Lys has a four-carbon chain.

Once again, the UV-visible spectra (Figure 6d) are generally consistent with the TEM results. When lysine is used as the major cross-linker, Cys:Lys < 1, one absorbance peak ranging from 510 to 550 nm dominates the spectrum. This is expected when the Au chain cross-section is larger or is composed of several particles, and also for the formation of linear aggregates (Figure 6a).[12] We did not observe any absorbance attributable to discrete Au colloids in the region of 500 nm, as was observed for Au nanorods[22] and Au linear aggregates.[21] This is because in the Cys-capped Au samples the size of the Au particle is less than 4 nm. When Cys predominates, Cys:Lys > 1, there remains a weak (vestigial) hump in the spectrum that correlates with an "oval" (not perfectly spherical) aggregate morphology. For Cys in large excess (Cys:Lys > 4) the spectrum is indistinguishable from that seen in Figure 3, representative of truly spherical aggregates.

Effect of functionally related cross-linking agents of varying chain length: To explore the importance of the molecular di-

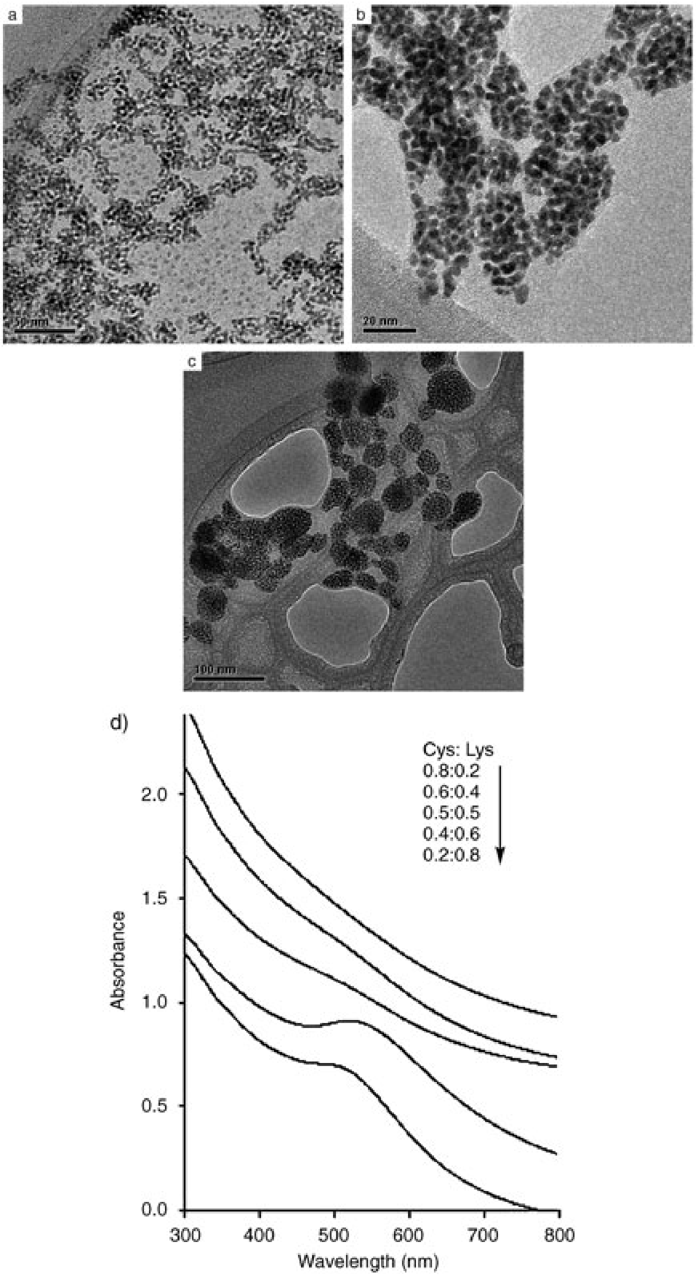

Figure 6. TEM images of Au colloid aggregates in the presence of different Cys:Lys ratios. a) 0.2:0.8, black bar represents 50 nm; b) 0.6:0.4, black bar represents 20 nm; c) 0.8:0.2, black bar represents 100 nm. All end-point pH values were close to 9.0. d) UV-visible spectra of Au aggregates.

mensions of the cross-linking agent, a series of chemically similar (SH-containing) organic acids of varying chain length, from 3-mercaptopropionic acid to 16-mercaptohexadecanoic acid, were mixed with Cys in a 1:1 ratio. The presence of capping agents of a similar chain length to Cys resulted in spherical aggregates with lower cohesion than was the case with Cys alone (Figure 7a). The use of very long-chain organic acids (Figure 7b) resulted in the formation of almost no spherical aggregates. This phenomenon can be explained according to the difference in electrostatic repulsion between the Au colloids. The SH-containing molecules have one terminal COOH group, which can be dissociated in conditions of high pH. Introduction of these molecules onto the Au colloid surface leads to a marked increase in the electrostatic repulsion between the colloids. When the chain length of the SH-containing molecules is similar to the length of the Cys molecules, the repulsion between the terminal COO^- groups is relatively weak, and the Cys molecules still have a chance to cross-link with the Au colloids. Because the SH-containing molecules, such as 16-mercaptohexadecanoic acid, are much longer than the Cys molecules, the repulsion begins to hinder the association of the Au colloids, even if they are not close to one other. This proves that the presence of Cys is necessary to facilitate the accumulation of well-ordered spherical aggregates of Au, and in addition, it suggests that the appropriate adjustment of surface charge, or the selection of a combination of various cross-linkers, will enable the aggregation state and morphology of the Au nanoparticles to be tailored and modified for valuable future applications.

Conclusion

We have demonstrated the formation of spherical aggregates of Au colloids by using Cys as a capping agent under appropriate conditions; pH 7–10 and gold:cysteine molar ratios from 1:0.5–1:2. The aggregate size can be adjusted by changing the concentrations of components; for 3–10 mM solutions of Au and Cys, very large spherical aggregates are formed, but these are unstable and more readily precipitated. The use of mixtures of Cys and Lys in varying proportions changes the aggregate morphology from a linear to a spherical form. Introduction of other SH-containing organic acids as capping agents of varying chain length may also influence the state and degree of aggregation in a systematic manner. The Au spherical aggregates of intermediate size (30–80 nm) produced in this work have a high stability, even at room temperature, and are readily dispersed in water.

Experimental Section

All chemicals were purchased from Sigma-Aldrich and used as received. In a typical room temperature synthesis, aqueous $HAuCl_4$ (10 mL, 1 mM) was mixed with aqueous cysteine solution (1.0 mL, 10 mM; Au:Cys = 1:1), and sufficient aqueous NaOH (0.2 M) was added to give the desired end-point pH value. Next, $NaBH_4$ (176 μL, 0.1 M) was added under vigorous stirring. At acidic pH (<4), the solution initially turned black, followed by rapid and extensive precipitation. At intermediate pH (6.5–11) a brown or dark brown solution developed that remained stable for several weeks.

UV-visible spectra were recorded by using a UV-2550 Spectrophotometer (Shimadzu) after preliminary dilution (1:1) with deionized water. TEM measurements were conducted by using a TECAI TF20 SuperTwin (200 kV) electron microscope, whereby a drop of solution was placed onto a Cu grid and dried in air.

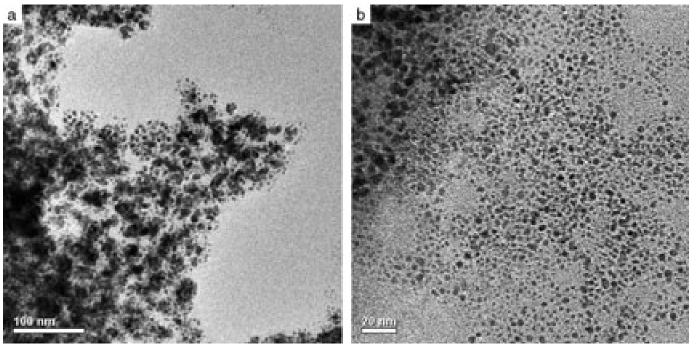

Figure 7. TEM images of Au colloid aggregates in the presence of mixtures of Cys and SH-containing organic molecules of various carbon chain lengths as capping agents. a) Cys with 3-mercaptopropionic acid (1:1), white bar represents 100 nm; b) Cys with 16-mercaptohexaxanoic acid (1:1), white bar represents 20 nm.

Acknowledgements

The authors would like to thank the Agency for Science, Technology, and Research in Singapore (A-STAR) for internal funding, and the kind support of Dr. P. K. Wong.

---

[1] a) P. L. Anelli, N. Spencer, J. F. Stoddart, *J. Am. Chem. Soc.* **1991**, *113*, 5131–5133; b) A. P. Alivisatos, P. F. Barbara, A. W. Castleman, J. Chang, D. A. Dixon, M. L. Klein, G. L. Mclendon, J. S. Miller, M. A. Ratner, P. J. Rossky, S. I. Stupp, M. E. Thompson, *Adv. Mater.* **1998**, *10*, 1297–1336.

[2] D. Feldheim, The Electrochemical Society Interface Fall Meeting, **2001**, 22–25.

[3] a) C. A. Mirkin, R. L. Letsinger, R. C. Mucic, J. J. Storhoff, *Nature* **1996**, *382*, 607–609; b) R. Elghanian, J. J. Storhoff, R. C. Mucic, R. L. Letsinger, C. A. Mirkin, *Science* **1997**, *277*, 1078–1081.

[4] a) S. Mann, W. Shenton, M. Li, S. Connolly, D. Fitzmaurice, *Adv. Mater.* **2000**, *12*, 147–150; b) W. Shenton, S. A. Davis, S. Mann, *Adv. Mater.* **1999**, *11*, 449–452; c) C. M. Niemeyer, W. Bürger, J. Peplies, *Angew. Chem.* **1998**, *110*, 2391–2395; *Angew. Chem. Int. Ed.* **1998**, *37*, 2265–2268.

[5] J. P. Novak, L. C. Brousseau III, F. W. Vance, R. C. Johnson, B. I. Lemon, J. T. Hupp, D. L. Feldheim, *J. Am. Chem. Soc.* **2000**, *122*, 12029–12030.

[6] B. L. Frankamp, A. K. Boal, V. M. Rotello, *J. Am. Chem. Soc.* **2002**, *124*, 15146–15147.

[7] T. B. Norsten, B. L. Frankamp, V. M. Rotello, *Nano Lett.* **2002**, *2*, 1345–1348.

[8] A. K. Boal, F. Ilhan, J. E. DeRouchy, T. Thurn-Albrecht, T. P. Russel, V. M. Rotello, *Nature* **2000**, *404*, 746–748.

[9] J. J. Shiang, J. R. Heath, C. P. Collier, R. J. Saykally, *J. Phys. Chem. B* **1998**, *102*, 3425–3430.

[10] S. Cobbe, S. Connoly, D. Ryan, L. Nagle, R. Eritja, D. Fitzmaurice, *J. Phys. Chem. B* **2003**, *107*, 470–477.

[11] M. Brust, D. Bethell, D. J. Schiffrin, C. J. Kiely, *Adv. Mater.* **1995**, *7*, 795–797.

[12] a) Z. Y. Zhong, S. Patskovskyy, P. Bouvrette, J. H. T. Luong, A. Gedanken, *J. Phys. Chem. B* **2004**, *108*, 4046–4052; b) Y. L. Xu, R. T. Wang, *Phys. Chem. Earth* **1998**, *58*, 3931–3948.

[13] a) M. C. Daniel, D. Astruc, *Chem. Rev.* **2004**, *104*, 293–346; b) Z. Y. Zhong, K. B. Male, J. H. T. Luong, *Anal. Lett.* **2003**, *36*, 3097–3118.

[14] J. D. Grunwaldt, C. Kiener, C. Wögerbauer, A. Baiker, *J. Catal.* **1999**, *181*, 223–232.

[15] T. Jensen, L. Lelly, A. Lazarides, G. C. Schatz, *J. Cluster Sci.* **1999**, *10*, 295–317.

[16] a) P. B. Johnson, R. W. Christy, *Phys. Chem. B* **1972**, *6*, 4370–4379; b) Y. L. Xu, *Appl. Opt.* **1997**, *36*, 9496–9508.

[17] a) R. G. Freeman, K. C. Grabar, K. J. Allsion, R. M. Bright, J. A. Davis, A. P. Guthrie, M. B. Hommer, M. A. Jackson, P. C. Smith, D. G. Walter, M. J. Natan, *Science* **1995**, *267*, 1629–1631; b) V. L. Colvin, M. C. Schlamp, A. P. Alivisatos, *Nature* **1994**, *370*, 354–357; c) K. C. Grabar, P. C. Smith, M. D. Musick, J. A. Davis, D. G. Walter, M. A. Jackson, A. P. Guthrie, M. J. Natan, *J. Am. Chem. Soc.* **1996**, *118*, 1148–1153; d) K. C. Grabar, K. A. Allison, B. E. Baker, R. M. Bright, K. R. Brown, R. G. Freeman, A. P. Fox, C. D. Keating, M. D. Musick, M. J. Natan, *Langmuir* **1996**, *12*, 2353–2361.

[18] a) X. Peng, J. Wickham, A. P. Alivisatos, *J. Am. Chem. Soc.* **1998**, *120*, 5343–5344; b) K. Naka, H. Itoh, Y. Tampo, Y. Chujo, *Nano Lett.* **2002**, *2* 1183–1186.

[19] K. Naka, H. Itoh, Y. Tampo, Y. Chujo, *Langmuir* **2003**, *19*, 5546–5549.

[20] a) N. Kimizuka, T. Kunitake, *Adv. Mater.* **1996**, *8*, 89–91; b) T. Yonezawa, K. Yasui, N. Kimizuki, *Langmuir* **2001**, *17*, 271–273.

[21] Z. Y. Zhong, J. Luo, T. P. Ang, J. Highfield, J. Lin, A. Gedanken, *J. Phys. Chem. B* **2004**, *108*, 18119–18123.

[22] Y. Niidome, K. Nishioka, H. Kawasaki, S. Yamada, *Chem. Commun.* **2003**, 2376–2377.

Received: May 27, 2004
Revised: November 22, 2004
Published online: January 18, 2005